Available online at www.sciencedirect.com
SciVerse ScienceDirect
Physics Procedia 29 (2012) 55 – 61
Physics Procedia

The Int. Conf. on Luminescence & Optical Spectroscopy of Condensed Matter 2011

Photoluminescence Properties of $Li_6Gd(BO_3)_3:Tb^{3+}$ under VUV / UV excitation

Feng Zhang[a], Yuhua Wang[a,*], Ye Tao[b]

[a] *Department of Materials Science, School of Physical Science and Technology, Lanzhou University, Lanzhou 730000, People's Republic of China*
[b] *Laboratory of Beijing Synchrotron Radiation, Institute of High Energy Physics, Chinese Academy of Sciences, Beijing 100049, People's Republic of China*

Received 25 July 2011; accepted 25 August 2011

Abstract

A series of phosphors $Li_6Gd_{1-x}(BO_3)_3:xTb^{3+}$ ($0 \le x \le 1$) was prepared by a conventional solid-state reaction method and their photoluminescence properties under VUV/UV excitation were demonstrated. For the excitation spectrum, the host-related absorption band, *f-f* and *f-d* transitions of Gd^{3+} and Tb^{3+}, charge transfer of $O^{2-} \rightarrow Gd^{3+}$ and $O^{2-} \rightarrow Tb^{3+}$ were assigned. In $Li_6Gd(BO_3)_3:Tb^{3+}$, visible quantum cutting through downconversion was observed upon Tb^{3+} $4f^8$-$4f^75d^1$ excitation and host excitation. The quantum cutting process was demonstrated combining a possible model.

PACS: 78.20.-e

Keywords: photoluminescence; downconversion; $Li_6Gd(BO_3)_3$

1. Introduction

The photoluminescence properties of rare earth ions in different oxysalt hosts in the VUV/UV range have attracted much attention due to their practical application [1-5]. When excited at VUV/UV light, few oxide phosphors have shown the potential application due to their weak absorption in the VUV/UV range or low energy transfer efficiency from VUV/UV photon to visible photon. To obtain high quantum conversion efficiency, an efficient method is via quantum cutting. It was reported that quantum cutting could be realized in an oxide with the band gap large enough [6].

The optical gap (Eg) of $Li_6Gd(BO_3)_3$ is large [7] to accommodate levels of rare earth ions. $Li_6Gd(BO_3)_3$ belongs to the monoclinic crystal system with $P2_1/c$ (Z=4) as the space group. [8] The structure unit of $Li_6Gd(BO_3)_3$ consist of BO_3 triangle panels, distorted GdO_8, LiO_4, and LiO_5 polyhedra. The Gd-O tetragonal prisms, connecting to one another by common edges along the direction oblique to the c axis, distribute in different layers in two-dimensional chains, which is shown in the insert of Fig.1. The smallest Gd-Gd distance in the same chain is 3.912 Å and that between different chains in the same layer is 8.846 Å. The Gd-Gd intrachain distance is rather short, while the corresponding interchain distance is about twice as large leading to the one-dimensional character of the crystal structure. Tb^{3+}-activated phosphors are usually excellent emitters of green light due to an effective excitation through the 4f-5d transitions covering a broad range of wavelengths and effective $^5D_4$-^7F_j transitions. [9] The ionic radii of Tb^{3+} (r_{Tb3+}=1.04 Å) is close to Gd^{3+} (r_{Gd3+}=1.06 Å) of $Li_6Gd(BO_3)_3$ host with eight-fold coordination environment [10]. The similar ionic radii values of Gd^{3+} and Tb^{3+} as well as the one-dimensional character of $Li_6Gd(BO_3)_3$ could permit the high-doping levels of Tb^{3+}.

In this study, we investigated the photoluminescence properties of Tb^{3+} activated $Li_6Gd(BO_3)_3$ which has a large band gap under VUV/UV light

* Corresponding author. Tel.: +86-931-8912772; fax: +86-931-8913554.
E-mail address: wyh@lzu.edu.cn.

doi:10.1016/j.phpro.2012.03.692

excitation. The results demonstrate that visible quantum cutting occurs in $Li_6Gd(BO_3)_3:Tb^{3+}$.

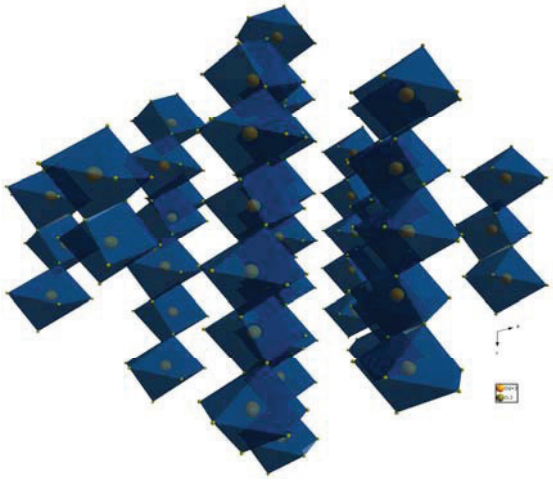

Fig. 1 Gd-O tetragonal prisms distributing in different layers in two-dimensional chains of $Li_6Gd(BO_3)_3$.

2. Experimental details

The compounds $Li_6Gd_{1-x}(BO_3)_3:xTb^{3+}$ ($0 \le x \le 1$) were prepared using mixtures of Li_2CO_3 (98%), HBO_3 (99.5%), Gd_2O_3 (99.99%), and Tb_4O_7 (99.99%), and fired in reducing mixtures at 660 °C for 6 h. The phase identification of samples was carried out by a Rigaku D/Max-2400 X-ray diffractometer with Ni-filter Cu Kα radiation.

Diffuse reflectance spectra were obtained by a $BaSO_4$ powder calibrated UV-VIS spectrophotometer (PE lambda 950). The UV luminescence spectra were measured by FLS920T fluorescence spectrophotometer. The VUV spectra were recorded at Beamline 4B8 in Beijing Synchrotron Radiation Facilities (BSRF) under dedicated synchrotron mode (2.5 GeV, 150-60 mA). All measurements were carried out at room temperature.

3. Results and discussion

3.1 Structural characterization

The XRD patterns of all the samples referred in this work were measured. The result indicates they are of a single phase. For representative, the patterns $Li_6Gd_{1-x}(BO_3)_3:xTb^{3+}$ (x=0, 0.2, 0.4, 0.6, 0.8, 1) are presented in Fig. 2. It is observed that the exhibited patterns can be well indexed based on the simulated pattern, showing they share the same phase.

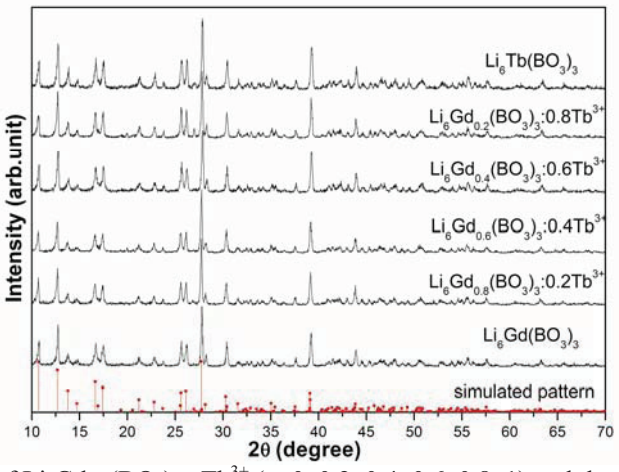

Fig. 2 The XRD patterns of $Li_6Gd_{1-x}(BO_3)_3:xTb^{3+}$ (x=0, 0.2, 0.4, 0.6, 0.8, 1) and the simulated XRD pattern.

3.2 UV-Vis diffuse reflectance spectra

Fig. 3 indicates the diffusion reflection spectrum of $Li_6Gd(BO_3)_3$, from which a drop trend from longer wavelength to shorter wavelength can be observed. In addition, two sharp absorption peaks at 274 and 312 nm are presented, which are due to the transitions from ground state level of Gd^{3+} ($^8S_{7/2}$) to ^6I_J and ^6P_J levels, respectively. The large-range optical absorption in $Li_6Gd(BO_3)_3$ may be caused by some uncertain defects produced in the synthesis process.

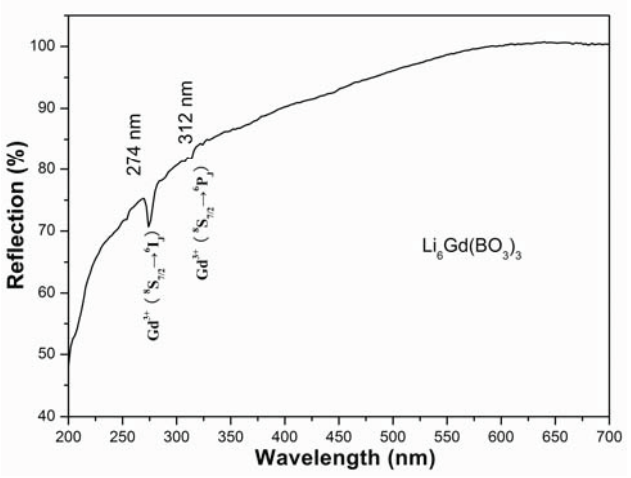

Fig. 3 Diffuse reflectance spectrum of $Li_6Gd(BO_3)_3$.

3.3 Spectroscopic properties of $Li_6Gd(BO_3)_3:Tb^{3+}$

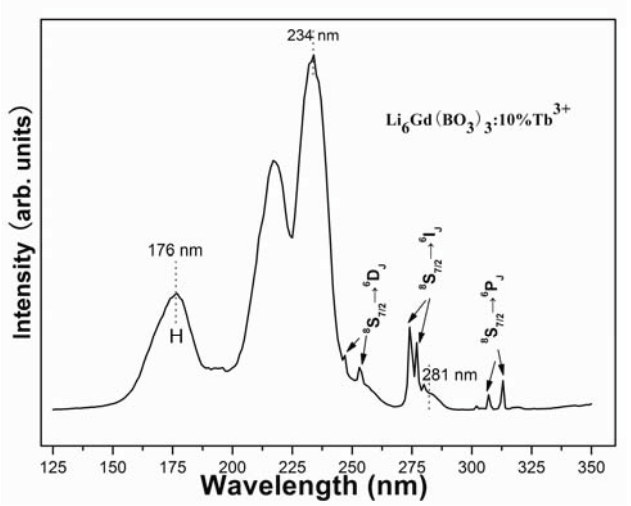

Fig. 4 VUV-UV excitation spectrum of the sample $Li_6Gd_{0.9}(BO_3)_3:0.1Tb^{3+}$.

The excitation spectrum of $Li_6Gd_{0.9}(BO_3)_3:0.1Tb^{3+}$ in the UV-VUV region was measured, which is indicated in Fig. 4. It can be observed that the spectrum is consisted of broad bands below 300 nm and some sharp lines around 253, 274 and 312 nm. The sharp lines around 253, 274 and 312 nm can be assigned to the Gd^{3+} transitions from the ground level $^8S_{7/2}$ to the excited state level ^6D_J, ^6I_J, ^6P_J, respectively. Many BO_3^{3-}-containing borates exhibit absorption around 140-180 nm [11-12], thus the broad band around 176 nm is determined to be host-related absorption band. Usually, $O^{2-}\rightarrow Tb^{3+}$ charge transfer band (CTB) and $O^{2-}\rightarrow Gd^{3+}$ CTB appear in the high energy region. Based on the Jørgensen empirical formula $E_{ct}(cm^{-1}) = [\chi opt(X) - \chi opt(M)] \times 30,000 cm^{-1}$ (1) [χopt(X) and χopt(M) are the optical electronegativities of the anion X and central metal cation M, respectively] [13], Using χopt(O)=3.1 [14], χopt(Gd)= 0.91 and χopt(Tb)=0.95 [15] into the formula above, the CTB of $O^{2-}\rightarrow Gd^{3+}$ and

$O^{2-}\rightarrow Tb^{3+}$ can be calculated to be 152 nm and 155 nm respectively. Thus, we consider the CTBs of $O^{2-}\rightarrow Gd^{3+}$ and $O^{2-}\rightarrow Tb^{3+}$ can be also included in the band at 176 nm. The spin-allowed (SA) $^7F_6$-^7D_J transitions (with higher energies and intensities) and spin-forbidden (SF) $^7F_6$-^9D_J transitions (with lower energies and intensities) will occur when one electron is promoted from the ground states $4f^8$ ($^7F_6$) to $4f^75d^1$ excitation levels [16], and the ^7D_J/^9D_J levels will be splitted due to the effect of crystal field. Thus, the transitions from $^7F_6$ to the ^7D_J/^9D_J sublevels will probably exist in the excitation spectrum, which results in the complicated *f-d* transitions of Tb^{3+}. Therefore, these additional bands at wavelength above 190 nm are related to the *f-d* transitions of Tb^{3+}. In order to assign the bands regioning from 190 nm to 290 nm, we adopt the following expression which was proposed by Dorenbos [17]:

$$D(A) = E(Ce, free) - E(Ln, A) + \Delta E^{Ln,Ce} \quad (2)$$

Here, E (Ce, free), which has been determined to be 49340 cm^{-1}, is defined as the energy of the first f-d transition of Ce^{3+} as a free (gaseous) ion. E (Ln, A) is the *f-d* energy difference of the lanthanide ions Ln^{3+} doped in compound A and $\Delta E^{Ln,Ce}$ is defined as the difference in *f-d* energy of Ln^{3+} with that of the first electric dipole allowed transition in Ce^{3+}. Using the value of D(A) in $Li_6Gd(BO_3)_3$, via, 20559 cm^{-1} [18], the position of *f-d* transitions Gd^{3+} is determined to be 134 nm which could be overlapped with band H, and the position of the lowest SA *f-d* transitions and SF *f-d* transitions of Tb^{3+} ions can be predicated to be 238±5 nm and 285±6 nm respectively, which are coincidence with the positions of the bands at 234 and 281 nm.

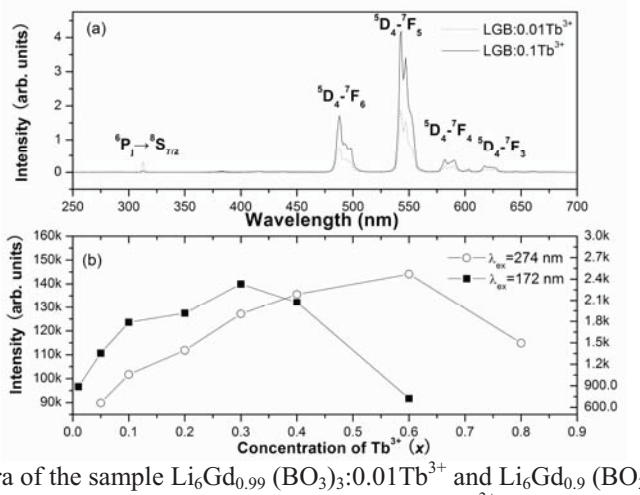

Fig. 5 (a) Emission spectra of the sample $Li_6Gd_{0.99}(BO_3)_3$:$0.01Tb^{3+}$ and $Li_6Gd_{0.9}(BO_3)_3$:$0.1Tb^{3+}$ upon 172 nm excitation, (b) the relationship between relative intensity of 543 nm and Tb^{3+}-doped concentration upon 274 and 172 nm excitation.

Upon 274 and 172 nm light excitation, the characteristic emission of Tb^{3+} from $^5D_4$-^7F_j transitions can be observed (shown as Fig. 5 (a)). It can be observed that the emission intensity at 543 nm increases with increasing Tb^{3+} content to x=0.6 (shown in the inset of Fig. 5 (b)), and then decreases excited at 274 nm. A possible reason for this high quenching concentration is the special structure of $Li_6Gd(BO_3)_3$ (shown in the insert of Fig. 1) which supports zigzag chains for Tb^{3+} restricting the energy migration to one dimension. Thus, the probability that the migrating excitation encounters one of the randomly distributed killer sites is reduced. Thus, the quenching concentration is determined to be 0.6 for excitation at 274 nm. When excited at 172 nm, the quenching concentration is considered to be 0.3. It has been reported that the high quenching concentration under VUV excitation has been related to the weak interaction between Tb^{3+} ion and host lattice [19], however, no direct evidence has been given. The reasons for the high quenching concentration need to be further studied. The different quenching properties under 274 and 147 nm light excitations imply that the quenching mechanisms mechanism under UV excitation is different from that under VUV excitation.

3.4 Quantum cutting and possible models in $Li_6Gd(BO_3)_3$:Tb^{3+}

To determine whether visible quantum cutting occurs in $Li_6Gd(BO_3)_3$:Tb^{3+}, we investigate the emission spectra of $Li_6Gd_{0.9}(BO_3)_3$:$0.1Tb^{3+}$ excited at 274 nm (the ^6I_J level of Gd^{3+}), 217 nm (the $4f^75d^1$ level of Tb^{3+}) and 172 nm (the host absorption) as a representation shown in Fig. 6. By scaling the spectra on the emission intensity for the

$^5D_3 \rightarrow {}^7F_5$ transition of Tb^{3+}. The emission intensity from level $^5D_4$ of Tb^{3+} excited at 217 and 172 nm is stronger than that excited at 274 nm. This result indicates that the quantum cutting indeed occurs in $Li_6Gd(BO_3)_3:Tb^{3+}$ excited at 217 and 172 nm.

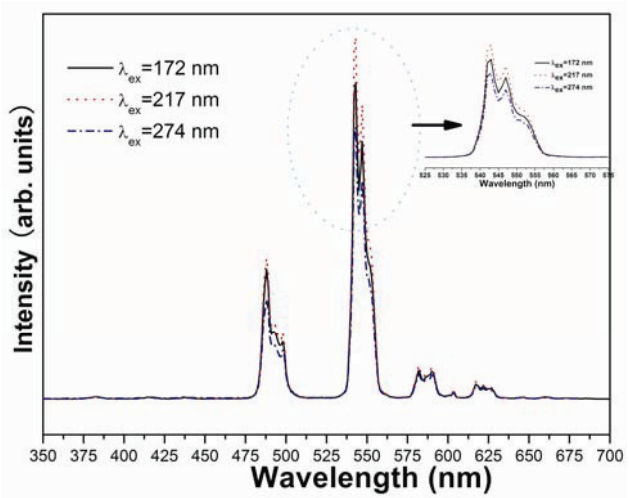

Fig. 6 Emission spectra of $Li_6Gd_{0.9}(BO_3)_3:0.1Tb^{3+}$ under 172, 217 and 274 nm light excitation. The spectra are scaled on the emission intensity for the $^5D_3 \rightarrow {}^7F_5$ transition of Tb^{3+}.

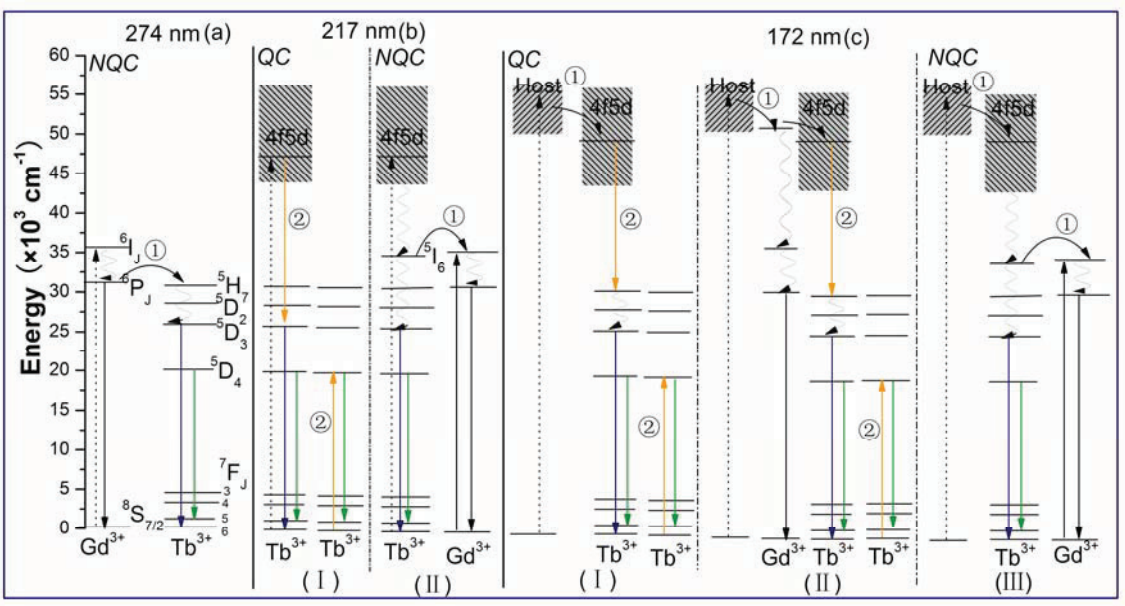

Fig. 7 Energy-level diagrams of visible quantum cutting through two-step energy transfer in $Li_6Gd(BO_3)_3:Tb^{3+}$ excited at (a) 274 nm, (b) 217 nm and (c) 172 nm. ① represents cross relaxation and ② represents direct energy transfer.

Fig.7 gives the possible energy level diagrams for $Li_6Gd(BO_3)_3:Tb^{3+}$ upon different excitation wavelengths. When $Li_6Gd(BO_3)_3:Tb^{3+}$ is excited at 274 nm, Gd^{3+} is pumped to ^6I_J level and then consume the energy via two ways shown in Fig. 7 (a). One is from ^6I_J level relaxed to $^6P_{7/2}$ state nonradiatively when direct energy transfer from $^6P_{7/2}$ to the neighboring Tb^{3+} ion. The other way is radiative relaxation of Gd^{3+} from $^6P_{7/2}$ to $^8S_{7/2}$. No visible QC occurs in this process. While upon excitation of $4f^8$-$4f^75d^1$ transition of Tb^{3+} at 217 nm, two possible cases take place (Fig. 7 (b)): in the first case, Tb^{3+} ion in $Li_6Gd(BO_3)_3:Tb^{3+}$ is excited from ground state to $4f^75d^1$ state, and then relaxes to an intermediated level $^5D_3$, then the released energy is transferred to a neighboring Tb^{3+} by cross relaxation resulting the excitation of Tb^{3+} to the level $^5D_4$ (process ②). This process results the extra green photons. The second way is that Tb^{3+} is relaxed from $4f^75d^1$ state to levels $^5D_3$ and $^5D_4$, the released energy is transferred to the neighboring Gd^{3+}.

176 nm is determined to be host-related absorption, thus it is considered that when $Li_6Gd(BO_3)_3:Tb^{3+}$ is excited at 176 nm, the energy is first absorbed by host and then is transferred from the host to a higher $4f^75d^1$ state of Tb^{3+}. Subsequently, three cases could occur: (1) the energy relaxes to a proper intermediated level of Tb^{3+}, and then the released energy is transferred to a neighboring Tb^{3+} by cross relaxation as observed in $Li_6Gd(BO_3)_3:Tb^{3+}$ upon excitation at 217 nm; (2) the energy relaxes to a proper intermediated level of Gd^{3+}, then energy transfer occurs from the intermediated level of Gd^{3+} to a higher $4f^75d^1$ state of Tb^{3+}, then occurs as case 1. The rest is relaxed to $^6P_{7/2}$ state nonradiatively and radiative relaxation of Gd^{3+} from $^6P_{7/2}$ to $^8S_{7/2}$ takes place; (3) the energy relaxes to a proper intermediated level of Tb^{3+}, and then relaxed from $4f^75d^1$ state to levels $^5D_3$ and $^5D_4$, the released energy is transferred to the neighboring Gd^{3+}.

4. Conclusion

The photoluminescence properties of a series of phosphors $Li_6Gd_{1-x}(BO_3)_3:xTb^{3+}$ ($0\leq x\leq 1$) under VUV/UV excitation were demonstrated. The host-related absorption band of $Li_6Gd_{1-x}(BO_3)_3:xTb^{3+}$ ($0.5\leq x\leq 1$) was determined to be 176 nm, and the *f-f* and *f-d* transitions of Gd^{3+} and Tb^{3+}, charge transfer of $O^{2-}\rightarrow Gd^{3+}$ and $O^{2-}\rightarrow Tb^{3+}$ were also assigned in the excitation spectrum. In $Li_6Gd(BO_3)_3:Tb^{3+}$, visible quantum cutting through downconversion was observed upon both Tb^{3+} $4f^8$-$4f^75d^1$ and host excitation.

5. Acknowledgments

This work is supported by National Science Foundation for Distinguished Young Scholars (Grant no. 50925206); National Natural Science Foundation of China (Grant no. 10874061) and the Doctoral Program of Higher Education (Grant no. 200807300010).

6. References

[1] F. Shen, D. He, H. Liu and J. Xu, VUV excitation properties of $LnZr(BO_3)_2$:Re (Ln=Ba, Sr; Re=Eu, Tb), J. Lumin. 122-123 (2007) 973-975.
[2] J. Wang, Z. Zhang, M. Zhang, Q. Zhang, Q. Su and J. Tang, The energy transfer from Eu^{2+} to Tb^{3+} in $Ca_{10}K(PO_4)_7$ and its application in green light emitting diode, J. Alloys Compd. 488 (2009) 582-585.
[3] R. Sankar, Efficient green luminescence in Tb^{3+}-activated borates, $A_6MM'(BO_3)_6$, Opt. Mater. 31 (2008) 268-275.
[4] V. Singh, S. Watanabe, T. K. Gundu Rao and H.Y. Kwak, Luminescence and defect centres in Tb^{3+} doped $LaMgAl_{11}O_{19}$ phosphors, Solid State Sci. 12 (2010) 1981-1987.
[5] Z. Wang, H. Liang, M. Gong and Q. Su, Novel red phosphor of Bi^{3+}, Sm^{3+} co-activated $NaEu(MoO_4)_2$, Opt. Mater. 29 (2007) 896-900.
[6] A. N. Belsky and J. C. Krupa, Luminescence excitation mechanisms of rare earth doped phosphors in the VUV range, Displays 19 (1999) 185-196.
[7] J. F. Rivas-Silva, A. Flores-Riveros and M. Berrondo, DFT Study of 1-D $Li_6Gd(BO_3)_3$, Int. J. Quantum Chem., 94, (2003)105-112.
[8] Y. Zhang, X. L. Chen , J.K. Liang and T. Xua, Phase relations of the system Li_2O–Gd_2O_3–B_2O_3 and the structure of a new ternary compound, J. Alloys Compd. 348 (2003) 314-318.
[9] A. Dobrowolska and E. Zych, Luminescence of Tb-doped $Ca_3Y_2(Si_3O_9)_2$ oxide upon UV and VUV synchrotron radiation excitation, J. Solid State Chem. 14 (2011) 1707-1714.
[10] R. D. Shannon, Handbook of Chemistry and Physics, Acta Cryst. A 32 (1976) 751-767.
[11] I.-E. Kwon, B.-Y. Yu, H. Bae, Y.-J. Hwang, T.-W. Kwon, C.-H. Kim, C.-H. Pyun and S.-J. Kim, Luminescence properties of borate phosphors in the UV/VUV region, J. Lumin. 87-89, (2000) 1039-1041.
[12] T. Jüstel, J.-C. Krupa and D. U. Wiechert, VUV spectroscopy of luminescent materials for plasma display panels and Xe discharge lamps, J. Lumin. 93, (2001) 179-189.
[13] C. K. Jørgensen, Electron transfer spectra of lanthanide complexes, Mol. Phys. 5 (1962) 271-277.
[14]R. Yavetskiy, M. Dubovik, A. Tolmachev and V. Tarasov, Radiation defects in $Li_6Gd(BO_3)_3:Eu^{3+}$ single crystals, phys. stat. sol. (c) 2 (2005) 268-271.
[15] Q. Su, J. Rare Earths (Special Issue), Optical electronegativity of lanthanide ions, in: Proceedings of the Second

Conference on Rare Earth Development and Application, 1991, 765-769.
[16] H. S. Yoo, W. B. Im, J. H. Kang and D. Y. Jeon, Preparation and photoluminescence properties of $YAl_3(BO_3)_4$: Tb^{3+}, Bi^{3+} phosphor under VUV/UV excitation, Opt. Mater. 31 (2008) 131-135.
[17] P. Dorenbos, J. Lumin. Predictability of 5d level positions of the triply ionized lanthanides in halogenides and chalcogenides, 87-89 (2000) 970-972.
[18] H. S. Kiliaan and G. Blasse, A study of the sensitizer in the luminescent systems, $(Y,Gd)_2O_2SO_4$:Bi,Tb and $Li_6(Y,Gd)(BO_3)_3$:S,Tb (S=Ce^{3+}, Pr^{3+} or Bi^{3+}, Mater. Chem. Phys. 18 (1987) 155-170.
[19] Z. Tian, H. Liang, W. Chen, Q. Su, G. Zhang and G. Yang, Efficient emission-tunable VUV phosphors $Na_2GdF_2PO_4$:Tb^{3+}, Opt. Express 17 (2009) 956-962.